Synthetic anti-BR3 antibodies that mimic BAFF binding and target both human and murine B cells

Chingwei V. Lee, Sarah G. Hymowitz, Heidi J. Wallweber, Nathaniel C. Gordon, Karen L. Billeci, Siao-Ping Tsai, Deanne M. Compaan, JianPing Yin, Qian Gong, Robert F. Kelley, Laura E. DeForge, Flavius Martin, Melissa A. Starovasnik, and Germaine Fuh

BR3, which is expressed on all mature B cells, is a specific receptor for the B-cell survival and maturation factor BAFF (B-cell–activating factor belonging to the tumor necrosis factor [TNF] family). In order to investigate the consequences of targeting BR3 in murine models and to assess the potential of BR3 antibodies as human therapeutics, synthetic antibody phage libraries were employed to identify BAFF-blocking antibodies cross-reactive to murine and human BR3, which share 52% identity in their extracellular domains. We found an antibody, CB1, which exhibits μM affinity for murine BR3 and very weak affinity for the human receptor. CB3s, an affinity-matured variant of CB1, has sub-nM affinity for BR3 from both species. Alanine scanning and crystallographic structural analysis of the CB3s/BR3 complex reveal that CB3s mimics BAFF by interacting with a similar region of the BR3 surface. Despite this similarity in binding epitopes, CB1 variants antagonize BAFF-dependent human B-cell proliferation in vitro and are effective at reducing murine B-cell populations in vivo, showing significant promise as therapeutics for human B-cell–mediated diseases. (Blood. 2006;108:3103-3111)

Introduction

BR3 (BAFF/BLyS receptor 3, also known as BAFF-R) was originally identified as a BAFF (B-cell–activating factor belonging to the tumor necrosis factor [TNF] family)–specific receptor important for B-cell survival in mice.[1,2] BR3 is expressed on all mature B cells and at very low levels on activated T cells.[3] BR3 expression is also maintained in many B-cell malignancies, such as non-Hodgkin lymphoma and chronic lymphocytic leukemia.[4] BAFF (also known as BLyS, TALL-1, zTNF-4, THANK, TNFSF13b) is a member of the TNF ligand superfamily and is capable of binding not only BR3, but also 2 other receptors, TACI (transmembrane activator and calcium modulator and cyclophilin ligand interactor) and BCMA (B-cell maturation antigen), both of which can also bind the related ligand APRIL (a proliferation-inducing ligand).[5,6] BAFF overexpression in mice induces B-cell hyperplasia and manifestations of autoimmune disease, whereas BAFF-knockout mice show near-complete absence of mature B cells. In humans, elevated levels of BAFF are found in a subset of patients with Sjögren syndrome, rheumatoid arthritis, and systemic lupus erythematosus and correlate with disease severity.[7-9] Elevated BAFF levels have also been reported in patients with diffuse large B-cell lymphoma and correlate with poorer clinical outcome.[4] Consequences of ligand-directed BAFF-blockade have been investigated in autoimmune disease models, showing significant efficacy in mouse models of lupus[10] and rheumatoid arthritis.[11,12] Several BAFF-targeted agents are currently being pursued in clinical development for both autoimmune disease and hematologic malignancies.[13-15]

However, BR3 is the principal receptor responsible for mediating BAFF-dependent B-cell survival effects.[1-3,16] Thus, targeting BR3 directly with an antibody, unlike the ligand-directed approaches, would disrupt the BAFF/BR3 axis specifically and leave BAFF free to signal through its other receptors. TACI was originally thought to act as an inhibitory receptor[17]; however, recent reports suggest that TACI could induce both positive and negative signals in B cells.[18,19] The function of BCMA is less clear; however, it appears to play a role in long-lived plasma cell survival.[20] Hence, the ability to compare agents specific for BR3 with those affecting other BAFF/receptor interactions in vivo will be valuable in furthering our understanding of this complex signaling pathway and may have important impacts on pharmaceutical development strategies.

Desired features of a therapeutic BR3 antagonistic antibody include the ability to bind BR3 with high affinity and prevent BAFF/BR3-binding, while *not* triggering BR3 signaling and B-cell survival on its own. Agonistic antibodies that activate other members of the TNF receptor family, due to the bivalent nature of immunoglobulin (IgG), have been described for TNFR, Fas, DR5, CD40, and CD137.[21-25] Further, developing a cross-reactive antibody that binds both murine (mBR3) and human BR3 (hBR3) (52% identity in their extracellular domains [ECDs][1,2]) would be useful, given that the in vivo effects and mechanisms of action of such an antibody could be evaluated in detail in murine models prior to clinical trials in humans. Antagonistic anti-hBR3

From the Departments of Protein Engineering, Assay and Automation Technology, and Immunology, Genentech Inc, South San Francisco, CA.

Submitted March 21, 2006; accepted June 21, 2006. Prepublished online as *Blood* First Edition Paper, July 13, 2006; DOI 10.1182/blood-2006-03-011031.

All of the authors are employees of Genentech Inc, and declare competing financial interests.

C.V.L., S.G.H., and L.E.D. designed and performed the experiments and wrote the paper; H.J.W., N.C.G., K.L.B., S.-P.T., D.M.C., J.P.Y., and Q.G. designed and performed the experiments; R.F.K. wrote the paper; and F.M., M.A.S., G.F. designed the experiments and wrote the paper.

The online version of this article contains a data supplement.

Reprints: Germaine Fuh or Melissa A. Starovasnik, Genentech Inc, Department of Protein Engineering, 1 DNA Way, South San Francisco, CA 94080; e-mail: gml@gene.com (G.F.) or star@gene.com (M.A.S.).

The publication costs of this article were defrayed in part by page charge payment. Therefore, and solely to indicate this fact, this article is hereby marked "advertisement" in accordance with 18 U.S.C. section 1734.

mAbs that inhibit BAFF-mediated B-cell proliferation in vitro have been described previously[3]; however, these mAbs were obtained by hybridoma technology and were not cross-reactive between species, which is not surprising given that mice remove self-reactive antibodies.[26] Here, we describe the use of phage-displayed synthetic antibody libraries[27] to identify a lead parental antibody and optimize its affinity to BR3 from both species, without prior knowledge of the binding paratope. Structural and functional studies of BR3 in complex with the cross-reactive antibody reveal the mechanism by which the antibody binds BR3 from both species and prevents BAFF binding. Finally, antagonistic activities of the phage-derived antibody are characterized in vitro with primary human B cells and in vivo in mice to reinforce the validity of such an antibody as a potential treatment for B-cell–mediated diseases.

Materials and methods

Phage library selection for BR3-binding clones

Phage-displayed synthetic antibody libraries were generated using oligonucleotide-directed mutagenesis in the 3 heavy chain complementarity-determining regions (CDRs) on a modified h4D5-encoding phagemid, pV350-4, as template, and described as Lib-3.[27] BR3-ECD was expressed in *Escherichia coli* and purified as described.[10] For initial selection with the naive libraries, mBR3-ECD and hBR3-ECD were immobilized on Maxisorp immunoplates (Nunc, Rochester, NY), and phage libraries were cycled through 4 rounds of binding selection.[27] Random clones selected from rounds 3 and 4 were picked and assayed to identify specific binders using phage enzyme-linked immunosorbent assay (ELISA). The V_H regions of selected clones were amplified by polymerase chain reaction (PCR) for sequencing.

Competition phage ELISA

Phage clones were propagated from a single colony by growing in 30 mL 2YT culture supplemented with carbenicillin and KO7 helper phage overnight at 30°C, purified, and assayed as described.[27,28] Phages (subsaturating concentration) were first incubated with increasing concentrations of mBR3-ECD or hBR3-ECD for 1 to 2 hours and transferred to mBR3-ECD–coated plates to capture the unbound phage. The amount of phage bound was measured with anti-M13 antibody horseradish peroxidase (HRP) conjugate (GE Healthcare, Piscataway, NJ) and developed with tetramethylbenzidine (TMB) (Kirkegaard and Perry Laboratories, Gaithersburg, MD) as substrate for approximately 5 minutes, quenched with 1.0 M H_3PO_4, and read spectrophotometrically at 450 nm wavelength as described.[27] Inhibitory concentration (IC_{50}) values were calculated as the concentration of soluble antigen that inhibited 50% of the phages from binding to immobilized antigen. For the BAFF blocking assay, phages were added to mBR3-coated wells in the presence of serial dilution of BAFF. Bound phages were measured with anti–M13-HRP.

Antibody phage libraries for affinity maturation

To create the phage template for affinity improvement, the GCN4 leucine zipper of the CB1 phagemid was first removed by Kunkel mutagenesis to provide a monovalent display format, and a stop codon (TAA) was incorporated in all CDR-L3 positions targeted for randomization. In the natural antibody-mimicking light chain library, the degeneracy design was as described.[27] In the soft randomization libraries, positions 91, 92, 93, 94, and 96 of CDR-L3, 31 to 33 of CDR-H1, 49 to 58 of CDR-H2, and the front half (95 to 100c), last half (99 to 100g) or the whole section (95 to 100g) of CDR-H3 except the 2 cysteines (positions 97, 100d) were coded with degenerate oligonucleotides. To achieve the soft randomization conditions, the mutagenic DNA was synthesized with 70-10-10-10 mixtures of bases favoring the wild-type nucleotides.[29] In the improvement of CB2, "stop" codons were again incorporated in the CDR-L3 of the template and "softer" randomization of CDR-H3 was included; mutagenic oligonucleotides were synthesized as 85-5-5-5 mixtures of bases.

Solution-phase sorting and screening for affinity improvement

A solution-phase sorting method was used to enhance the efficiency of affinity-based selection as described.[27] Phage libraries were incubated with biotinylated mBR3-ECD or hBR3-ECD for 2 hours at room temperature in phosphate-buffered saline (PBS) with 0.05% (vol/vol) Tween20 and 0.5% Superblock (Pierce, Rockford, IL). The mixture was diluted 5- to 10-fold with PTS and incubated with immobilized neutravidin for 5 to 10 minutes to capture phages bound to the biotinylated mBR3-ECD or hBR3-ECD. Libraries were cycled through 3 to 4 rounds of selection with decreasing concentrations of biotinylated mBR3-ECD or hBR3-ECD. In the last round of selection, 1000-fold excess of nonbiotinylated mBR3-ECD or hBR3-ECD was added to compete for binding at 37°C for 30 minutes before capturing on neutravidin-coated wells. A high-throughput, single-point competition ELISA was then used to screen for high-affinity clones as described.[30] Competition phage ELISAs with purified phages were used to identify affinity improvements.

Fab and IgG production

To generate Fab or IgG proteins for characterization, the variable domains of selected phage clones were cloned into vectors designed for Fab expression in *E coli* as described[27] or pRK5-based plasmid with human or murine light chain or heavy chain (human IgG1 or murine IgG2a) constant domain for transient IgG expression in Chinese hamster ovary (CHO) cells. Fab protein was generated by growing the transformed 34B8 *E coli* cells in AP5 medium at 30°C for 24 hours and purified using protein G affinity chromatography.[27] Full-length IgG proteins were purified using protein A, followed by ion exchange chromatography, and quantified by amino acid analysis.

Affinity measurements

Surface plasmon resonance (SPR) measurements (BIAcore-3000; BIAcore, Uppsala, Sweden) were used to determine the affinity of anti-BR3 Fabs. Carboxymethylated dextran biosensor chips (CM5; BIAcore) were activated with *N*-ethyl-*N*′-(3-dimethylaminopropyl)-carbodiimide hydrochloride and *N*-hydroxysuccinimide. BR3-ECD was added to achieve approximately 150 response units (RUs). Two-fold serial dilutions of anti-BR3 Fab (500 nM-3 nM) were injected in PBS with 0.05% Tween 20 at 25°C at a flow rate of 25 μL/min. Binding responses on immobilized mBR3-ECD or hBR3-ECD were corrected by subtracting the signal from a blank control flow cell. Association rates (k_{on}) and dissociation rates (k_{off}) were calculated using a simple one-to-one Langmuir fitting model (BIAcore Evaluation Software version 3.2). Equilibrium dissociation constants (K_D) were calculated as the ratio of k_{off} to k_{on}. For most Fabs, the K_D values determined were in general agreement with the phage IC_{50} values.

Competitive BAFF-binding ELISA on BR3-expressing cells

BHK cells transfected with full-length mBR3, or BJAB cells, which naturally express hBR3 on the cell surface, were seeded at 250 000 cells per well on Nunc round-bottom plates and kept on ice. Serial dilution of antibodies in cell-binding buffer (PBS with 0.5% BSA and 1% FBS [PBF]) were mixed with biotinylated-BAFF at 10 ng/mL. Mixtures were applied to the wells for binding 45 minutes on ice, cells were spun down at 300*g* for 5 minutes and washed 3 times with PBF. The streptavidin-HRP was added for 45 minutes on ice. The plates were washed, developed with TMB substrate for approximately 5 minutes, quenched with 1.0 M H_3PO_4 and read spectrophotometrically at 450 nm wavelength. IC_{50} values were calculated as the concentration of IgG that inhibit BAFF binding to 50% levels. The values reflect anti-BR3 antibody affinity but are highly dependent on the receptor density of the cells.

Epitope-mapping of human BR3 by shotgun-scanning mutagenesis

The construction of miniBR3 (residues 17-42) shotgun libraries, sorting strategy, and analysis were described previously.[31] The template was a

modified phagemid pW1205a that encodes an epitope tag (gD tag, amino acid sequence: MADPNRFRGKDLGG) fused to the N-terminus of the human miniBR3 DNA template with stop codons at the positions to be scanned, followed by the M13 major coat protein gene-8. Two libraries were generated. Library 1 included mutations at positions 17, 18, 20-23, 25, 27, 28, 30, and 33, while library 2 included mutations at positions 26, 29, 31, 34, and 36 to 42. Each library contained 2×10^9 members, allowing for complete representation of the theoretical diversity ($> 10^4$-fold excess).

Phages were subjected to 2 rounds of binding selection against the anti-BR3 mAbs (murine IgG2a) 9.1, 2.1, 11G9, and CB2 immobilized on 96-well Nunc Maxisorp immunoplates. mAbs 9.1[3] and 2.1 were kindly provided by Biogen Idec (Cambridge, MA). Forty-eight individual clones positive for binding the antibody target they were selected against were sequenced. Functional ratio *(F)* values describing the effects of mutation on binding were calculated as described previously using prior data of anti-gD antibody selection to normalize the effect of display efficiency.[32] Given the limited number of sequences evaluated, only *F* values representing a more than 10-fold change (ie, $F \geq 10$ or $F \leq 0.1$) are considered significant.

Protein purification and crystallization for structure determination

A BR3 expression construct was generated by cloning a gene fragment encoding S7-A54 of hBR3-ECD and a tyrosine at the amino-terminus (to add a cloning site) into XbaI/*Bam*HI sites of the expression vector, pET-32a (Novagen, San Diego, CA), which was modified to delete the S-Tag and enterokinase site. Residues V20 and L27 were mutated to mBR3 sequence (N20 and P27) to improve protein production efficiency.[33] Origami (DE3) competent cells (Novagen) transformed with pET32a-BR3-ECD were grown with isopropyl-β-D-thiogalactopyranoside (IPTG) induction overnight at 16°C. BR3 cell pellets were lysed in 20 mM CAPS, pH 9.7, 400 mM NaCl by microfluidization. Cell supernatant was eluted from a Ni-NTA agarose column (Qiagen, Valencia, CA) in buffer containing 50 mM imidazole. Protein was then passed over a S75 sizing column, the thioredoxin–His-tag was removed by thrombin cleavage, and untagged BR3 was further purified on an S75 sizing column. The expression and purification of CB3s- and CB2-Fab in *E coli* were as described.[27,28]

For complex formation for crystallization, BR3 and CB3s-Fab were mixed at a 3:1 molar ratio, and purified over a S75 sizing column in 20 mM MES, pH 6.0, 50 mM NaCl (Buffer A). Purified complex was concentrated to 20 mg/mL to 40 mg/mL in Buffer A and used for crystallization trials. Crystals grew by vapor diffusion at 19°C from sitting drops. Drops contained 2.1 μL protein solution and 2.9 μL citric acid pH 3.0, 24% PEG 3350, and 0.1 M Praseodymium (III) acetate over a reservoir of 24% PEG 3350. Crystals were cryoprotected by immersion in a solution of 8.4 mM MES, pH 6.0, 21 mM NaCl, 9 mM citric acid, pH 3.0, 24% PEG 3350, and 100 mM Praseodymium (III) acetate with 20% dextrose. CB2-Fab was purified as described for CB3s-Fab except that the buffer for the final column was 25 mM MES pH 6.0, 100 mM NaCl. The sample was concentrated to 11 mg/mL. Crystals were grown in hanging drops with a 1:1 ratio of protein to well solution consisting of 100 mM HEPES, pH 7.5, 20% PEG 10K, and then frozen in mother liquor with 25% PEG 400.

Crystallography

The CB2 crystals belong to space group P1. A 0.195 nm (1.95 Å) data set was collected at beamline 19ID at the Advanced Photon Source and processed with HKL software (HKI, Charlottesville, VA) (Table 2). The structure was solved by molecular replacement using the humanized 4D5 Fab (PDB code 1FVE). Final R and R_{free} are 19.9% and 23.3%, respectively, for 6417 protein atoms and 58 water molecules. The model has good stereochemistry; a Ramanchandran plot shows that 99% of all residues are in the most favored or additionally allowed regions, with only 7 residues in generously allowed or disallowed regions.[34] The CB3s-Fab/BR3 crystals belong to space group $I2_13$ with $a = 14.64$ nm (146.4 Å). A 0.26 nm (2.6 Å) data set was measured at beamline 5.0.1 at the Advanced Light Source and processed with HKL (Table 2). Calculation of the Matthew coefficient indicated that the asymmetric unit consisted of one CB3s-Fab/BR3 complex. The structure was solved by molecular replacement using the refined 0.195 nm (1.95 Å) crystal structure of CB2 and the program Amore (CCP4, Daresbury, England). Good density for BR3 and CDR-H3 were observed in the initial electron density maps. A model of BR3 from the BAFF/BR3 complex (PDB code 1P0T[35]) was manually positioned in the density. Then, the structure was refined with the program REFMAC5 (CCP4). The final R and R_{free} are 19.6% and 25.3%. The final model consists of the first 213 and 220 residues of the CB3s light and heavy chains, respectively, and variant hBR3 residues 13 to 39. The model has good stereochemistry, and a Ramanchandran plot shows that 98.7% of all residues are in the most favored or additionally allowed regions, with only 5 residues in generously allowed or disallowed regions.[34]

Paratope-mapping of CB3s by shotgun-scanning mutagenesis

The template for alanine and homologue shotgun-scanning libraries used a bicistronic CB3s-Fab–displaying phagemid containing the light chain fused C-terminally to a gD tag, and the heavy chain V_H and C_H1 fused to the C-terminal domain of the M13 minor coat protein P3 (cP3), with stop codons introduced at the positions to be scanned, as described.[36,37] Two rounds of selection were performed on immobilized hBR3 or mBR3 ECD, or anti-gD antibody, and approximately 96 positive clones were sequenced. The anti-gD sort serves to gauge the Fab protein folding and display efficiency since the heavy chain is fused to the phage coat, and displaying gD tag, which is fused to light chain, requires proper folding and association of the light chain and heavy chain. The results were tabulated in Figure S3 (available on the *Blood* website; see the Supplemental Materials link at the top of the online article) with *F* for m1 (alanine mutation), m4 (homologue mutation), and m2 and m3 (additional substitutions encoded by shotgun-alanine codons for F, H, L, I, K, M, N, Q, R, W, Y).

B-cell proliferation assays

Human B cells were isolated from peripheral blood mononuclear cells by positive selection using CD19 MACS magnetic beads (Miltenyi Biotec, Auburn, CA). To evaluate the antagonistic effects of anti-BR3 antibodies (all in hIgG1 format), B cells (1×10^5/well) were incubated with soluble recombinant BAFF (10 ng/mL) and an $F(ab')_2$ goat anti–human IgM (Fc-specific) antibody (4 μg/mL; Jackson ImmunoResearch, West Grove, PA) in the presence and absence of various concentrations of anti-BR3 antibody. The same assay format, with the exception that BAFF is omitted, was used to assess potential agonistic effects. B-cell proliferation was assessed at day 6 by adding Celltiter Glo (Promega, Madison, WI). The plates were then read in a luminometer after a 10-minute incubation at room temperature.

In vivo study

Six- to 8-week-old BALB/c mice (Jackson Laboratory, Bar Harbor, ME) were injected intravenously with 200 μg control mIgG2a antibody, BR3-Fc (made by fusing mouse BR3 extracellular domain with mouse IgG1 Fc fragment), or an Fc mutant (D265A/N297A) of CB2 (mouse IgG2a), named CB2-IgG*, which is incapable of binding Fcγ receptors.[38] During the duration of the experiment the serum concentration of both CB2-IgG* and BR3-Fc were significant (average blood concentrations at day 6 were 83.4 ± 9.8 μg/mL and 32.4 ± 5.4 μg/mL), consistent with the approximately 6-day and approximately 3-day half-lives for wild-type CB2-IgG and BR3-Fc determined previously in separate pharmacokinetic (PK) experiments (data not shown). Furthermore, serum concentrations maintained during in vivo experiments were on average 10- to 50-fold above the thresholds needed for B-cell reduction characterized in separate PK/pharmacodynamic (PD) studies (Q.G. and F.M., manuscript in preparation). At day 6, mice were killed; B cells, T cells, granulocytes, and macrophages were quantified in blood and spleen by flow cytometry using anti-B220, anti-CD3, anti-Gr1, and anti-CD11b antibodies (Becton Dickinson, Mountain View, CA); and values were analyzed using a standard statistical *t* test.

Table 1. Relative affinities of initial BR3 binding clones

	Phage IC_{50} (nM)		IgG EC_{50} (nM)	
Clones	mBR3	hBR3	mBR3	hBR3
CB1	1700	> 5000	50	> 2000
CB1a	> 5000	NB	20	NB
CB1b	> 5000	NB	NB	NB
CB1c	> 5000	NB	200	NB

Relative affinities for mBR3 and hBR3 ECD measured by competition phage ELISA or direct binding as purified IgG proteins to BR3-coated wells.

NB indicates no detectable binding.

Results

Discovery of a phage-derived anti-BR3 BAFF-blocking antibody

Synthetic antibody libraries that allow for bivalent display of Fab fragments on the M13 phage[27,36] were employed for initial identification of BR3-binding antibodies. The antibody libraries were generated by randomizing 17 residues in the heavy chain CDRs on the humanized anti-erbB2 antibody 4D5 (h4D5) template in a manner that mimics the diversities of natural antibodies. Four unique clones (CB1, CB1a, CB1b, CB1c) were identified by selecting for binding to mBR3-ECD; no clones were identified by selection for binding to hBR3. All 4 clones showed modest micromolar binding affinities to mBR3 in competition phage ELISA (Table 1); however, CB1 had the greatest ability to compete with BAFF for BR3-binding (Figure 1). Full-length IgG versions were generated to use increased avidity to detect weak binding. CB1-IgG was the only antibody showing any detectable binding to hBR3 (Table 1).

Affinity improvement for binding to both mBR3 and hBR3

To improve the affinity of CB1 for both murine and human BR3, 4 different combinations of CDR loops were targeted for randomization: L1/L2/L3, L2/L3/H1, L3/H3, and L3/H1/H2 (Figure 2A). The strategy of co-evolving several CDR loops together allows for simultaneous optimization of the CDR-antigen and CDR-CDR interactions, as it was observed previously that combining independently optimized CDRs often results in nonadditivity and reduced affinities.[39] CDR residues were selected for randomization using a structure-guided strategy of choosing surface-accessible residues.[27] In designing the diversity for targeted positions, we used restrictive codons for residues in CDR-L1, -L2, and -L3 to mimic the diversity in natural antibodies as described,[27] or a strategy of "soft randomization" for CDR-H1, -H2, -H3, and -L3,[40,41] in which the selected residues were mutated to non–wild-type residues or maintained as wild type at an approximately 50:50 frequency. The CDR-H3 loop of CB1 contains 15 residues including a pair of cysteines. The cysteine pair was excluded from randomization, as mutation of these residues was found to entirely disrupt the already weak binding (data not shown).

Through stringent selection for binding to mBR3 or hBR3, followed by screening for cross-reactivity, 3 unique variants (CB2, CB2a, CB2b) were isolated from the CDR-L3/H3 library and one variant (CB2c) from the CDR-L2/L3/H1 library by selecting against mBR3 (as before, hBR3 selections yielded no enrichment). All variants showed improved affinity to mBR3, but with different extents of cross-reactivity (Figure 2B). CB2 with alterations in CDR-L3 (Y92R, T93I) and CDR-H3 (S99N, S100R, $V100_aL$, $R100_bG$, $G100_cV$, $A100_gG$) appeared to be the best clone, exhibiting single-digit nM affinity (ELISA, IC_{50}) for mBR3 and hBR3, representing a more than 200- and 1000-fold affinity improvement, respectively (Figure 2B, Figure S1). Note that selection for improved binding to mBR3 also resulted in improved binding to hBR3, suggesting that CB2 recognizes a region of BR3 conserved across species.

To further improve the affinity of CB2, the CDR loop combinations of L3/H3 or L3/H1/H2 were randomized using a similar strategy. Interestingly, the CDR-L3/H3 library did not show enrichment in this round of affinity selection, suggesting that further mutations of these 2 loops are mainly disruptive. In contrast, many affinity-improved variants were identified from the CDR-L3/H1/H2 library, based on selecting for binding to either hBR3 or mBR3. Among the variants, CB3, mutated at CDR-L3 (R92Q, T94S) and CDR-H1 and -H2 (N32S, I51V, T52L, D54V, N56F), showed improved binding to mBR3 and hBR3 by 3- and 10-fold, respectively. However, a potential N-linked glycosylation site was generated in the CB3 CDR-H1 sequence for residues 31-33 (N-S-S). Hence, mutant CDR-H1-N31S, named CB3s, was engineered to remove the glycosylation site, and showed improved binding compared with CB3, when expressed from mammalian cells. CB3s-Fab bound mBR3 and hBR3 with affinities of 1 nM and 0.6 nM (K_D), respectively (Figure 2B).

Mapping anti-BR3 binding sites on hBR3

The 26-residue core of hBR3 (miniBR3, residues 17-42) contains a well-structured β-hairpin, and was shown to maintain equivalent BAFF-binding affinity as the full-length BR3-ECD.[10] Similarly, we find that CB2-Fab binds equally well to miniBR3 as to the full-length ECD (data not shown). To further define the antibody-binding site on BR3, shotgun alanine–scanning phage libraries of miniBR3, constructed previously for mapping the BAFF-binding epitope on BR3,[31] were employed to assess the contribution of individual BR3 residues for binding CB2. As a comparison, we also map the binding sites of 3 hybridoma-derived anti-hBR3 antibodies (11G9, 2.1, and 9.1; Figure 3A). These antibodies also block BAFF-binding and have epitopes lying within miniBR3 (data not shown). In shotgun alanine–scanning mutagenesis, the preference for the wild-type residue over alanine at each scanned position, corrected for display differences, provides a measure of the contribution of that residue to ligand binding. A value for the normalized functional ratio (F) of more than 1 indicates the wild-type residue is preferred for ligand binding and a value less than 1 indicates that an alanine substitution improves binding.

A set of substitutions (F25A, D26A, V33A, A34G) showed significant loss ($F \geq 10$) in binding for all 4 antibodies and BAFF. While this could indicate that these residues contribute directly to the interaction with all of the binders, a more plausible explanation is that these substitutions disrupt the conformational integrity of the BR3 molecule and thus indirectly affect binding. Indeed, the F25A mutation was previously identified as one that likely destabilizes

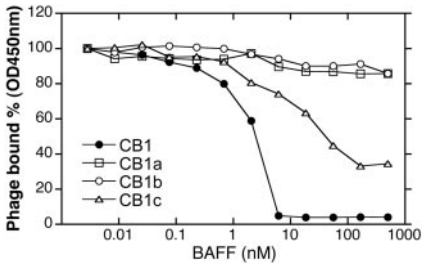

Figure 1. Characterization of initial BR3 Fab phage selectants. Phage binding to mBR3-coated ELISA wells in the presence of BAFF.

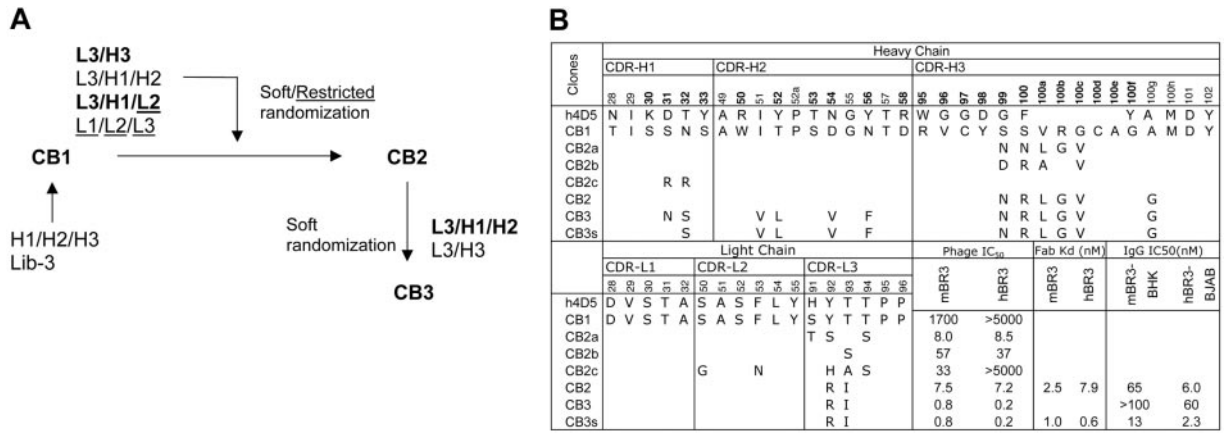

Figure 2. Affinity improvement of CB1. (A) Flow chart of CB1 affinity maturation. Combinations of CDR loops were diversified in different libraries by soft randomization (see "Materials and methods") or restricted randomization mimicking natural antibody diversities (underlined). The CDR combinations shown in bold text indicate the libraries from which improved binders were isolated. (B) Amino acid sequences of CB1 CDRs as deduced from DNA sequencing are aligned with the template of the synthetic antibody libraries, h4D5. The positions randomized in the libraries are in bold. Alterations in the affinity-improved variants are shown with their affinities measured as Fab-phage IC_{50} values in competition ELISA, as Fab K_D values measured with SPR technology (BIAcore), or as IgG protein IC_{50} values competing with BAFF for binding to mBR3-(BHK) or hBR3-(BJAB) expressing cells, as described in "Materials and methods."

the BR3 structure.[31] Other substitutions affect only a subset of binders and are likely to reveal specific contacts that define distinct epitopes as highlighted on the structure of miniBR3 in Figure 3B. Note that the hybridoma-derived antibodies appear to use nonconserved residues, accounting for their lack of cross-reactivity between species. Strikingly, the binding site for CB2 closely mimics that for BAFF, with L28A and V29A each showing significant loss in binding; L28 and V29 form the tip of the $_{26}$DLLVRH$_{31}$ β-turn (or "DxL(V/L) motif"), previously shown to be the key structural and functional contact with BAFF[10,31,35] (Figure 3C). These residues are conserved in hBR3 and mBR3, and similarly, BAFF itself is capable of binding tightly to both hBR3 and mBR3.[2]

As BAFF also interacts with 2 other receptors, BCMA and TACI, which contain similar conserved sequences and structures in their respective β-turn regions (Figure 3C),[42,43] we tested CB2-IgG for binding human and murine BCMA and TACI. No detectable binding was found for either receptor (Figure S2). Thus, CB2

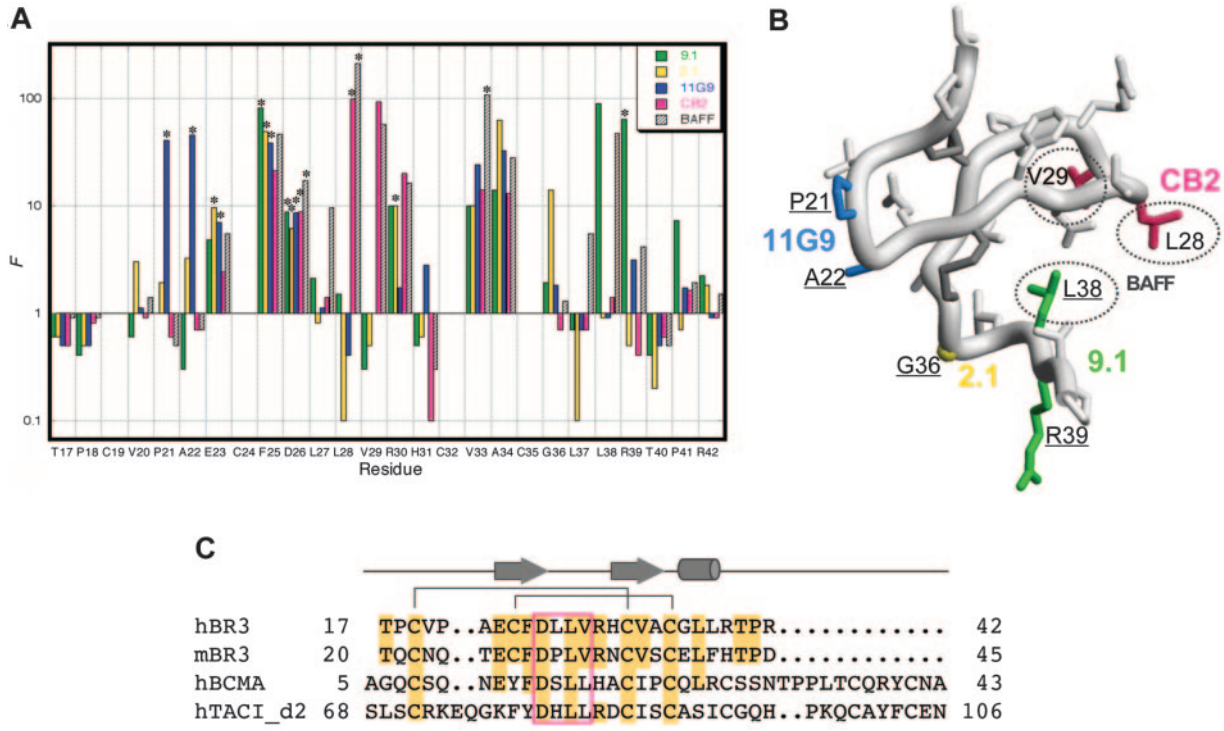

Figure 3. Mapping binding sites on BR3. (A) Shotgun alanine–scanning mutagenesis of miniBR3 for binding to antibodies and BAFF. The normalized functional ratios *(F)* observed for each of the scanned positions in BR3 obtained from sequences of positive clones after selection for binding to CB2-IgG, BAFF,[31] or hybridoma-derived antibodies 9.1, 2.1, and 11G9. Bars with an asterisk above them indicate values that represent a lower limit because alanine was not observed at these positions. (B) Functional epitopes mapped on the structure of hBR3 (1P0T[35]). Distinct antibody determinants ($F > 10$) based on shotgun alanine–scanning are highlighted for each BR3-binder by coloring corresponding side chains as in panel A; key BAFF-binding residues are circled. Residues that affect a majority of binders are not colored as they likely affect binding indirectly. Residues that differ between hBR3 and mBR3 are underlined. (C) Sequence alignment of the BAFF-binding cysteine-rich domains of hBR3, mBR3, h-BCMA, and h-TACI. Secondary structure and disulfide-bonding pattern of BR3 are shown. Residues identical to hBR3 are shaded. The conserved DxL(V/L) motif is boxed.

Table 2. Crystallographic statistics

	CB2-Fab	CB3s-Fab/BR3 complex
Data collection		
Space group	P1	$I2_13$
Cell dimensions		
a,b,c, Å	38.7, 73.0, 90.0	146.4
α, β, γ, °	109.4, 101.0, 96.1	
Resolution, Å*	50-1.95 (2.02-1.95)	50-2.60 (2.69-2.60)
R_{sym}*†	0.074 (0.366)	0.064 (0.440)
I/GI*	6.9 (1.9)	11.7 (3.7)
Completeness, %*	98.0 (91.8)	100 (100)
Redundancy	3.36	11.36
Asymmetric unit	2 CB2 Fab fragments	1 CB3s-BR3 complex
Refinement		
Resolution, Å	30-1.95	30-2.6
No. reflections	63 790	15 951
R_{work}/R_{free}‡	19.9/23.3	19.6/25.3
No. atoms		
Protein	6417	3448
Ligand/ion	0	0
Water	58	27
RMS deviations		
Bond lengths, Å	0.010	0.010
Bonded Bs, Å^2	2.7	2.5
Bond angles, °	1.12	1.25
Ramachandran plot, % residues		
Most favored	90.6	90.5
Additionally allowed	8.4	8.2
Generously allowed	0.6	1.0
Disallowed	0.4	0.3

RMS indicates root mean square. To convert Å to nm, multiply by 0.1.

*Numbers in parentheses refer to the highest resolution shell.

†$R_{sym} = \Sigma |I - \langle I \rangle| / \Sigma I$. $\langle I \rangle$ is the average intensity of symmetry related observations of a unique reflection.

‡$R = \Sigma |F_o - F_c| / \Sigma F_o$. R_{free} is calculated as R, but for 10% of the reflections that have been excluded from refinement.

cross-reacts with human and murine orthologues of BR3, but does not bind other BAFF receptors.

Structure of the CB3s/hBR3 complex

To investigate the molecular basis of BAFF-blocking and cross-species binding of CB1 variants, the crystal structure of CB2-Fab alone and a complex between CB3s-Fab and an hBR3 variant (residues 7-54) were determined at 0.195 nm (1.95 Å) and 0.26 nm (2.6 Å) resolutions, respectively (Table 2). Variant hBR3 has 2 changes relative to hBR3 (L27P and V20N). These changes replace human residues with their murine counterparts and result in improved BR3 expression and folding efficiency,[33] while maintaining high-affinity BAFF and CB3s binding. The structure of CB2-Fab alone adopts a typical Fab conformation except for CDR-H3, which is disordered beyond the disulfide. In the CB3s/BR3 complex, the entire CDR-H3 loop is well-ordered, suggesting that this long loop becomes stabilized by BR3 binding. In this structure, the BR3 DxLV motif binds CB3s in a manner very similar to its interaction with BAFF (Figure 4); the interaction centers on L28 and V29 of BR3, which binds in a hydrophobic pocket on CB3s created by the juncture of the CDR-H2 and -L3 loops (Figure 5A). D26 of BR3 forms a salt bridge to R95 of CDR-H3, which mimics the salt bridge between D26 and BAFF residue R265 observed in structures of BAFF with different receptors or receptor fragments (Figure 4).[31,35,43,44] Unlike the relatively focused epitope between BR3 and BAFF, which buries approximately 10 nm^2 (1000 Å^2) in accessible surface area on complex formation, the CB3s/hBR3 interface is much larger (~16 nm [1600 Å^2]). In the BAFF/BR3 structure, the only residues that significantly contact BAFF outside of the β-turn region are V33 and L38. In contrast, residues 31 to 38 all contact CB3s-Fab. Thus, CB3s blocks BAFF by using an epitope that completely encompasses the BAFF-binding site on BR3.

Mapping hBR3 and mBR3 binding sites on CB3s

Next, we wanted to understand how CB3s accommodates binding to both hBR3 and mBR3, which differ substantially in sequence. Shotgun alanine–scanning mutagenesis, which varies CB3s CDR residues between wild-type or alanine, and shotgun homologue–scanning, which varies CDR residues between wild-type or a homologous amino acid, were performed to measure the contribution of individual side chains, or the requirement for a specific side chain, respectively.[37] *F* values indicating the preference of the wild-type residue over the mutation for each varied position were calculated and tabulated (Figure S3). Results from alanine scanning for both hBR3 and mBR3 binding are shown on the structure of CB3s-Fab with coloring according to the functional importance for each residue (Figure 5B-C). Overall, the paratope mapped by shotgun-scanning mutagenesis is highly consistent with the structural interface (Figure 5A). Whereas some of the residues showing disruptive mutations do not make direct contact with BR3, most of

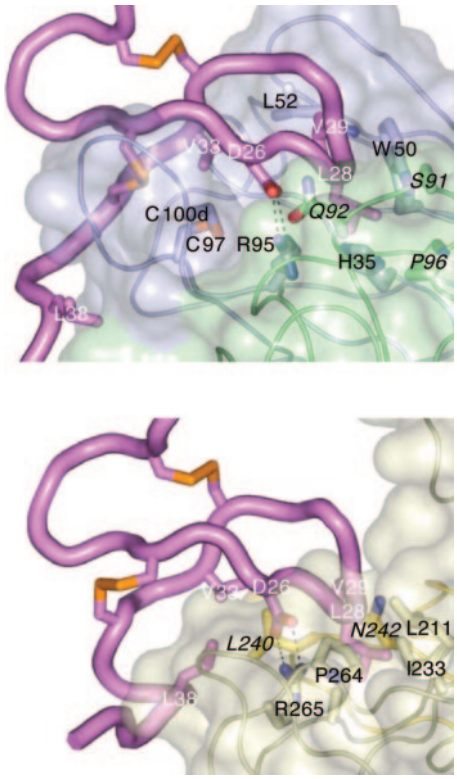

Figure 4. CB3s mimics BAFF binding to BR3. Structure of the CB3s-Fab/BR3 complex (top) compared with the BAFF/BR3 complex (bottom; 1OTZ/1P0T[35]). BR3 (magenta) is shown in the same orientation in both complexes. The tip of the BR3 β-hairpin (L28/V29) points into a cavity at the junction of light (green) and heavy (blue) chains on CB3s (transparent surface models, selected side chain shown), or at the junction of 2 BAFF monomers (light and dark gold), with BR3 D26 forming a salt bridge with an arginine side chain in each complex. CB3s contact residues are labeled in black, light chain residues are in italic; key BAFF-binding residue side chains of BR3 are shown and labeled in white.

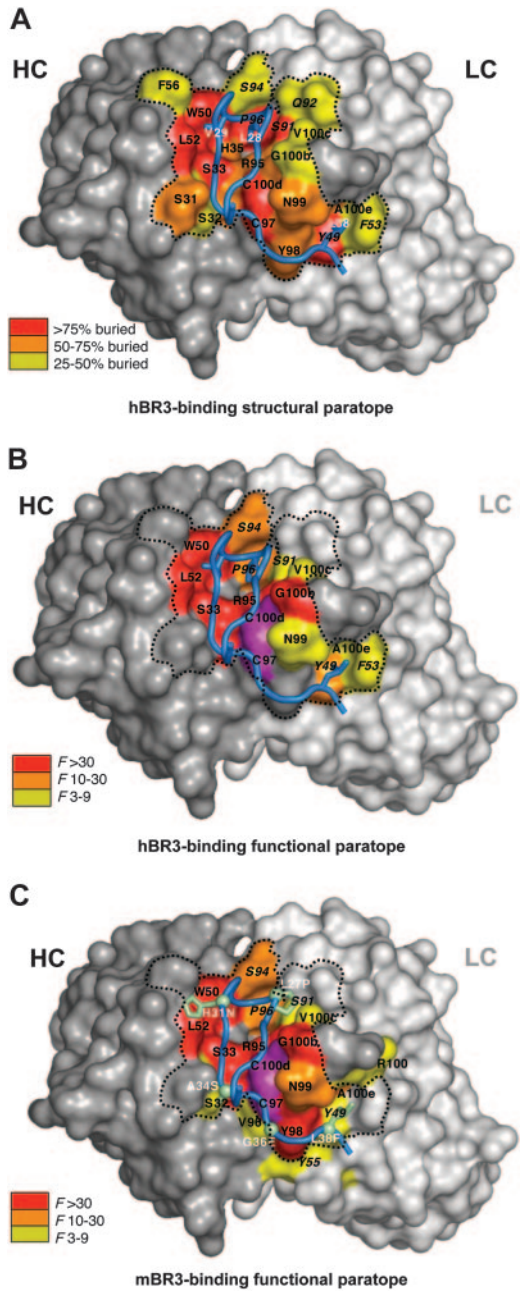

Figure 5. Structural and functional paratopes of CB3s for hBR3 and mBR3 binding. (A) The CB3s CDR binding surface of heavy (gray) and light (white) chains with structural contacts colored according to the extent buried by BR3. Residues are labeled using the same format as in Figure 4. (B) Residues that contribute energetically to binding hBR3 or (C) mBR3 are mapped on the structure of CB3s with color coding according to their importance as indicated by shotgun alanine–scanning *F* values. In panel C, side chains for hBR3 residues that differ in mBR3 are shown and labeled (white) with the human-to-murine substitution. The functionally important disulfide in CDR-H3 is colored magenta. The dotted line depicts the perimeter of the main structural paratope.

the highly important side chains ($F > 10$) make extensive contact with the receptor.

A set of residues, which are similarly important for binding to hBR3 and mBR3 ($F > 10$ when substituted by alanine) make up a common "hot spot,"[45] composed of residues from CDR-H1 (S33), CDR-H2 (W50, L52), CDR-H3 (R95, G100b, G100f), and CDR-L3 (S94, P96), plus the cysteine pair in CDR-H3 (Figure 5B-C). Other than G100f in CDR-H3, whose role is likely indirect, this common hot spot interacts with the β-hairpin of BR3 (residues 25-33). Even homologous substitutions at most of these positions are highly disruptive (Figure S3). Notably, most of these hot spot residues already exist in the parental clone CB1, suggesting that this region confers the main binding energy in the initial clone before affinity improvement. Three residues, L52 (CDR-H2), G100b (CDR-H3), and S94 (CDR-L3), altered during subsequent affinity maturation, likely contribute to improving binding affinities. The differences between human and murine BR3 in this portion of the interface (L27P, H31N; human vs murine residue) appear to be accommodated equally.

In contrast, a set of CDR-H3 residues of CB3s (Y98, N99, R100, A100e) that interact with the "C-terminal tail" of BR3 (residues 34-38) are functionally more important for mBR3- than for hBR3-binding, whereas some CDR-L2 residues (Y49, F53) interacting with the same segment of BR3 are functionally more important for hBR3- than for mBR3-binding (Figure 5B-C, Figure S3). Interestingly, the alteration of these residues in CDR-H3 appears to be the key to switch the specificity from the mostly mBR3-selective CB1 to the equally cross-reactive CB2; CB2c, retaining the CB1 CDR-H3, is not nearly as cross-reactive to hBR3 as CB2.

The property of cross-species binding by CB3s appears to be achieved first by using a common hot spot binding interaction with conserved residues in the BR3 β-hairpin, in a manner similar to BAFF, and second by being able to also accommodate the rest of the molecule and differentially distribute the binding energy toward residues that differ between species. CB1 was initially discovered by panning for binders to mBR3; thus, the observation that the binding site appears to "fit" mBR3 better than hBR3 is not surprising. As the binding site evolved, mutations appeared to have been selected that better accommodate hBR3 binding rather than introducing new hBR3-specific interactions.

Antagonism of BAFF-dependent activities in vitro

BAFF was previously shown to costimulate primary human B-cell proliferation in the presence of anti-IgM[46]; such BAFF-dependent proliferation could be blocked by BAFF-receptor fusion proteins or anti-BR3 mAbs.[3] To establish whether these cross-reactive antibodies trigger or block BR3 signaling, a similar assay format was used. Both CB2-IgG and CB3s-IgG were found to antagonize BAFF-dependent human B-cell proliferation with IC_{50} values of 1 nM and 0.03 nM, respectively, consistent with their relative affinities (Figure 6A). Importantly, no agonistic activity was observed with CB2-IgG and CB3s-IgG on their own in the presence of anti-IgM (Figure 6B). In contrast, a humanized version of 2.1-IgG, one of the hybridoma-derived antibodies, was found to agonize B-cell proliferation in the absence of BAFF, showing the potential for different outcomes depending on the characteristics of different BR3 antibodies.

BAFF/BR3 blockade in vivo

To determine whether an anti-BR3 BAFF-blocking antibody is effective in reducing B-cell populations in vivo, a variant of CB2-IgG with mutations in the Fc region that ablate effector function (CB2-IgG*)[38] was tested in BALB/c mice and compared with effects due to BR3-Fc treatment. This antibody mutant was chosen in order to compare directly the effects of in vivo BAFF/BR3 blockade based on targeting the receptor rather than targeting the ligand, without the confounding effects of engaging Fc receptors and potentially inducing Fc-mediated cytotoxicity by

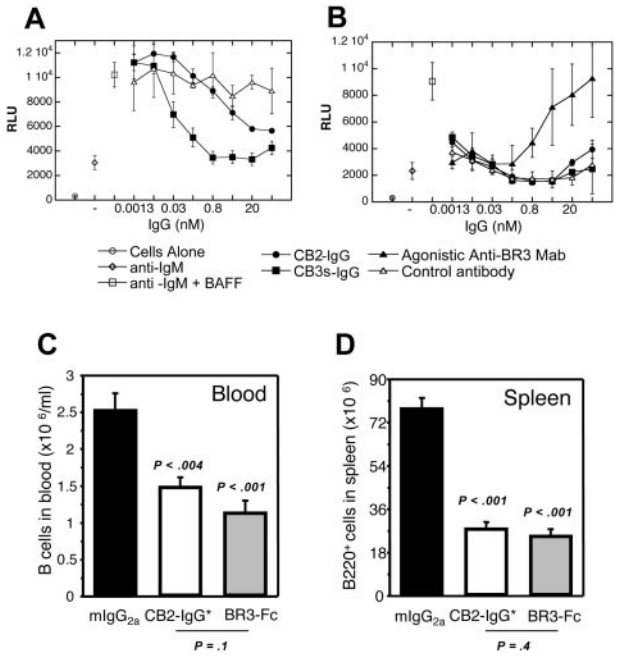

Figure 6. Antagonistic properties of CB1 variants in vitro and in vivo. (A) CB2-IgG and CB3s-IgG inhibit BAFF/anti-IgM costimulated primary human B-cell proliferation as described in "Materials and methods." (B) Human B cells were treated with anti-IgM and increasing concentrations of control, CB2-IgG, CB3s-IgG, or a hybridoma-derived agonistic anti-BR3 antibody control. Only the agonistic antibody showed dose-dependent B-cell proliferation. (C) Blood and (D) spleen B-cell numbers in groups of 5 Balb/C mice 6 days after treating with control, BR3-Fc, and CB2-IgG* (IgG with ablated Fc-mediated effector function). Error bars indicate standard error of the mean (SEM) of 5 mice per group.

the anti-BR3 antibody. Prior to in vivo administration, the specificity of the CB2 antibody for BR3 and B-lineage cells was confirmed through histology on tissue panels and general flow cytometry. Whereas CB2 reacted clearly with B-cell areas in tissues and B-lineage cells, no other binding activity was detected (Figure S4 and data not shown). Six days after in vivo administration of these molecules, B cells in both blood and spleen were reduced to a similar level by CB2-IgG* and BR3-Fc (Figure 6C-D), suggesting that blockade of the BAFF/BR3 survival pathway whether via targeting the ligand or receptor results in a similar decrease in survival of the B-cell compartment, emphasizing the key role that BR3 plays in BAFF-dependent survival. No differences in absolute cell number counts were seen in any other cell type analyzed including spleen and blood T cells, blood granulocytes, and spleen macrophages (data not shown). Although the Fc backbones of the 2 reagents were different (mouse IgG1 for BR3-Fc and mouse IgG2a* Fc mutant for CB2), their serum concentrations during the experiment were similar and remained significantly above target saturation and B-cell reduction thresholds, allowing for direct comparison between the 2 strategies of BAFF blockade (see "Materials and methods" for details). Thus, this significant reduction in B-cell populations shows that CB2-IgG* efficiently blocks the survival signal mediated through the BAFF/BR3 pathway in normal mouse B cells in vivo.

Discussion

Herein we describe an antagonistic BR3 antibody, CB1, identified from antibody phage libraries by initially screening for a Fab-displaying phage clone that competed for mBR3 binding to BAFF. CB1 was then improved to bind hBR3 and mBR3 with equally high affinity by altering residues from several CDR loops. This property of cross-species binding is a benefit of generating antibodies via in vitro panning processes that clearly use different rules for selecting epitopes compared with hybridoma technologies.[28] We show that the improved CB1 variants, CB2 and CB3s, bind BR3 in a manner that mimics how the ligand BAFF binds BR3 both structurally and functionally, indicating that the BR3 epitope that evolved in vivo for binding its natural biologic partner is also a "hot spot" targeted by in vitro selection. The cross-species high-affinity binding of CB3s is due mainly to interactions with this conserved hot spot. However, additional residue substitutions selected during affinity maturation were necessary to better accommodate other regions of the receptor, where sequence differences occur between species. This mechanism of high-affinity binding and specificity determination is reminiscent of other protein-protein interactions where the energetic hot spot, which is often conserved, and the site determining specificity are distinct.[47]

Clinical development of human antibody therapeutics typically use surrogate antibodies in animal disease models to gain a more in-depth understanding of the mechanism and therapeutic potential of modulating particular targets. Advantageously, such surrogate antibodies are unnecessary for CB2 and CB3s due to their cross-reactive properties. We show that the phage-derived anti-BR3 antibodies can block BAFF-dependent B-cell survival both in vitro and in vivo, despite the finding that these antibodies interact with BR3 in a manner similar to that invoked by BAFF. Furthermore, CB2-IgG*, which targets the BR3 receptor directly, is as effective at reducing B-cell populations in vivo as BR3-Fc, an agent that instead targets the ligand BAFF. This in vivo activity of CB2 demonstrates the validity of targeting BR3 for the treatment of B-cell–mediated disorders. Finally, antibodies against BR3 have the further potential to target B cells for destruction via antibody-dependent cytotoxic mechanisms, such as ADCC and CDC, similar to mechanisms used by anti-CD20 antibodies such as Rituximab[48] (comprehensive characterization of anti-BR3 mechanisms of action in vivo to be described elsewhere). The potential to combine in one therapeutic agent both BAFF/BR3-survival blockade and antibody-mediated cytotoxicity mechanisms provides an exciting alternative, and potentially a complementary approach to existing CD20-targeted strategies[14] for the treatment of B-cell–mediated diseases, such as hematologic malignancies and autoimmune disorders.[14,49]

Acknowledgments

We thank Abraham de Vos, Sachdev S. Sidhu, and Dimitry Danilenko for helpful discussions, and members of the Pathology, DNA synthesis, DNA sequencing, N-terminal sequencing, and mass spectrometry groups at Genentech for technical support. The Advanced Photon Source, and the Advanced Light Source at Lawrence Berkeley National Laboratory, are supported by the U.S. Department of Energy, Office of Science, Office of Basic Energy Sciences under contract nos. W-31-109-ENG-38 and DE-AC03-76SF00098, respectively. Coordinates for CB2-Fab and CB3s-Fab/BR3 complex structures are available from the RCSB Protein Data Bank with accession codes 2HFF and 2HFG, respectively.

References

1. Thompson JS, Bixler SA, Qian F, et al. BAFF-R, a newly identified TNF receptor that specifically interacts with BAFF. Science. 2001;293:2108-2111.
2. Yan M, Brady JR, Chan B, et al. Identification of a novel receptor for B lymphocyte stimulator that is mutated in a mouse strain with severe B cell deficiency. Curr Biol. 2001;11:1547-1552.
3. Ng LG, Sutherland APR, Newton R, et al. B cell-activating factor belonging to the TNF family (BAFF)-R is the principal BAFF receptor facilitating BAFF costimulation of circulating T and B cells. J Immunol. 2004;173:807-817.
4. Novak AJ, Grote DM, Stenson M, et al. Expression of BLyS and its receptors in B-cell non-Hodgkin lymphoma: correlation with disease activity and patient outcome. Blood. 2004;104: 2247-2253.
5. Schneider P. The role of APRIL and BAFF in lymphocyte activation. Curr Opin Immunol. 2005;17: 282-289.
6. Mackay F, Browning JL. BAFF: a fundamental survival factor for B cells. Nature Rev Immunol. 2002;2:465-475.
7. Cheema GS, Roschke V, Hilbert DM, Stohl W. Elevated serum B lymphocyte stimulator levels in patients with systemic immune-based rheumatic diseases. Arthritis Rheum. 2001;44:1313-1319.
8. Groom J, Kalled SL, Cutler AH, et al. Association of BAFF/BLyS overexpression and altered B cell differentiation with Sjögren's syndrome. J Clin Invest. 2002;109:59-68.
9. Zhang J, Roschke V, Baker KP, et al. Cutting edge: a role for B lymphocyte stimulator in systemic lupus erythematosus. J Immunol. 2001; 166:6-10.
10. Kayagaki N, Yan M, Seshasayee D, et al. BAFF/BLyS receptor 3 binds the B cell survival factor BAFF ligand through a discrete surface loop and promotes processing of NF-kB2. Immunity. 2002; 17:515-524.
11. Gross JA, Dillon SR, Mudri S, et al. TACI-Ig neutralizes molecules critical for B cell development and autoimmune disease: impaired B cell maturation in mice lacking BLyS. Immunity. 2001;15:289-302.
12. Wang H, Marsters SA, Baker T, et al. TACI-ligand interactions are required for T cell activation and collagen-induced arthritis in mice. Nat Immunol. 2001;2:632-637.
13. Baker KP, Edwards BM, Main SH, et al. Generation and characterization of LymphoStat-B, a human monoclonal antibody that antagonizes the bioactivities of B lymphocyte stimulator. Arthritis Rheum. 2003;48:3253-3265.
14. Martin F, Chan AC. B cell immunobiology in disease: evolving concepts from the clinic. Annu Rev Immunol. 2006;24:467-496.
15. Vugmeyster Y, Seshasayee D, Chang W, et al. A soluble BAFF antagonist, BR3-Fc, decreases peripheral blood B cells and lymphoid tissue marginal zone and follicular B cells in cynomolgus monkeys. Am J Pathol. 2006;168:476-489.
16. Shulga-Morskaya S, Dobles M, Walsh ME, et al. B cell-activating factor belonging to the TNF family acts through separate receptors to support B cell survival and T cell-independent antibody formation. J Immunol. 2004;173:2331-2341.
17. Seshasayee D, Valdez P, Yan M, Dixit VM, Tumas D, Grewal IS. Loss of TACI causes fatal lymphoproliferation and autoimmunity, establishing TACI as an inhibitory BLyS receptor. Immunity. 2003; 18:279-288.
18. Castigli E, Wilson S, Scott S, et al. TACI and BAFF-R mediate isotype switching in B cells. J Exp Med. 2005;201:35-39.
19. Salzer U, Chapel H, Webster A, et al. Mutations in TNFRSF13B encoding TACI are associated with common variable immunodeficiency in humans. Nat Genet. 2005;37:820-828.
20. O'Connor BP, Raman VS, Erickson LD, et al. BCMA is essential for the survival of long-lived bone marrow plasma cells. J Exp Med. 2004;199: 91-97.
21. Menegazzi R, Cramer R, Patriarca P, Scheurich P, Dri P. Evidence that tumor necrosis factor alpha (TNF) induced activation of neutrophil respiratory burst on biologic surface is mediated by the p55 TNF receptor. Blood. 1994;84:287-293.
22. Gonzalez-Cuadrado S, Lopez-Armada MJ, Gomez-Guerrero C, et al. Anti-Fas antibodies induce cytolysis and apoptosis in cultured human mesangial cells. Kidney Int. 1996;49:1064-1070.
23. Sun Y, Chen HM, Subudhi SK, et al. Costimulatory molecule-targeted antibody therapy of a spontaneous autoimmune disease. Nat Med. 2002;8:1256-1258.
24. Ichikawa K, Liu W, Zhao L, et al. Tumoricidal activity of a novel anti-human DR5 monoclonal antibody without hepatic cytotoxicity. Nat Med. 2001; 7:954-960.
25. Schwabe RF, Hess S, Johnson JP, Engelmann H. Modulation of soluble CD40 ligand bioactivity with anti-CD40 antibodies. Hybridoma. 1997;16:217-226.
26. Carnemolla B, Neri D, Castellani P, et al. Phage antibodies with pan-species recognition of the oncofoetal angiogenesis marker fibronectin ED-B domain. Int J Cancer. 1996;68:397-405.
27. Lee CV, Liang W-c, Dennis MS, Eigenbrot C, Sidhu S, Fuh G. High-affinity human antibodies from phage-displayed synthetic Fab libraries with a single framework scaffold. J Mol Biol. 2004;340: 1073-1093.
28. Fuh G, Wu P, Liang W-C, et al. Structure-function studies of two synthetic anti-vascular endothelial growth factor Fabs and comparison with the Avastin-Fab. J Biol Chem. 2006;281:6625-6631.
29. Gallop M, Barrett R, Dower W, Fodor S, Gordon E. Applications of combinatorial technologies to drug discovery, 1: background and peptide combinatorial libraries. J Med Chem. 1994;37:1233-1251.
30. Sidhu SS, Li B, Fellouse F, Eigenbrot C, Fuh G. Phage-displayed antibody libraries of synthetic heavy chain complementarity determining regions. J Mol Biol. 2004;338:299-310.
31. Gordon NC, Pan B, Hymowitz SG, et al. BAFF/BLyS receptor 3 comprises a minimal TNF receptor-like module that encodes a highly focused ligand-binding site. Biochemistry. 2003;42:5997-5983.
32. Weiss GA, Watanabe CK, Zhong A, Goddard A, Sidhu SS. Rapid mapping of protein functional epitopes by combinatorial alanine scanning. Proc Natl Acad Sci U S A. 2000;97:8950-8954.
33. Pelletier M, Thompson JS, Qian F, et al. Comparison of soluble decoy IgG fusion proteins of BAFF-R and BCMA as antagonists for BAFF. J Biol Chem. 2003;278:33127-33133.
34. Laskowski RA, MacArthur MW, Moss DS, Thornton JM. PROCHECK: a program to check the stereochemical quality of protein structures. J Appl Crystallogr. 1993;26:283-291.
35. Kim HM, Yu KS, Lee ME, et al. Crystal structure of the BAFF-BAFF-R complex and its implications for receptor activation. Nat Struct Biol. 2003;10: 342-348.
36. Lee CV, Sidhu SS, Fuh G. Bivalent antibody phage display mimics natural immunoglobulin. J Immunol Methods. 2004;284:119-132.
37. Vajdos FF, Adams CW, Breece TN, Presta LG, de Vos AM, Sidhu SS. Comprehensive functional maps of the antigen-binding site of an anti-ErbB2 antibody obtained with shotgun scanning mutagenesis. J Mol Biol. 2002;320:415-428.
38. Shield RL, Namenuk AK, Hong K, et al. High resolution mapping of the binding site on human IgG1 for FcgRI, FcgRII, FcgRIII, and FcRn and design of IgG1 variants with improved binding to the FcgR. J Biol Chem. 2001;276:6591-6604.
39. Yang W, Green K, Ping-sweeney S, Briones A, Burton D, Barbas III C. CDR walking mutagenesis for the affinity maturation for a potent human anti-HIV-1 antibody into the picomolar range. J Mol Biol. 1995;254:392-403.
40. Dennis MS, Roberge M, Quan C, Lazarus RA. Selection and characterization of a new class of peptide exosite inhibitors of coagulation factor VIIa. Biochemistry. 2001;40:9513-9521.
41. Wrighton NC, Farrell FX, Chang R, et al. Small peptides as potent mimetics of the protein hormone erythropoietin. Science. 1996;273:458-463.
42. Hymowitz SG, Patel DR, Wallweber HJA, et al. Structures of APRIL-receptor complexes: Like BCMA, TACI employs only a single cysteine-rich domain for high-affinity ligand binding. J Biol Chem. 2005;280:7218-7227.
43. Zhang G. Tumor necrosis factor family ligand-receptor binding. Curr Opin Struct Biol. 2004;14: 154-160.
44. Liu Y, Hong X, Kappler J, et al. Ligand-receptor binding revealed by the TNF family member TALL-1. Nature. 2003;423:49-56.
45. Clackson T, Wells JA. A hot spot of binding energy in a hormone-receptor interface. Science. 1995;267:383-386.
46. Moore PA, Belvedere O, Orr A, et al. BLyS: member of the tumor necrosis factor family and B lymphocyte stimulator. Science. 1999;285:260-263.
47. Li W, Keeble AH, Giffard C, James R, Moore GR, Kleanthous C. Highly discriminating protein-protein interaction specificities in the context of a conserved binding energy hotspot. J Mol Biol. 2004;337:743-759.
48. Gong Q, Ou Q, Ye S, et al. Importance of cellular microenvironment and circulatory dynamics in B cell immunotherapy. J Immunol. 2005;174:817-826.
49. Martin F, Chan AC. Pathogenic roles of B cells in human autoimmunity: insights from the clinic. Immunity. 2004;20:517-527.